INTERNATIONAL JOURNAL FOR NUMERICAL METHODS IN FLUIDS
Int. J. Numer. Meth. Fluids 2006; **50**:1369–1379
Published online 31 October 2005 in Wiley InterScience (www.interscience.wiley.com). DOI: 10.1002/fld.1093

On the geometric conservation law in transient flow calculations on deforming domains

Ch. Förster[1,*,†], W. A. Wall[2,‡] and E. Ramm[1,§]

[1]*Institute of Structural Mechanics, University of Stuttgart Pfaffenwaldring 7, 70550 Stuttgart, Germany*
[2]*Chair of Computational Mechanics, Technical University of Munich, Boltzmannstraße 15, 85747 Garching, Germany*

SUMMARY

This note revisits the derivation of the ALE form of the incompressible Navier–Stokes equations in order to retain insight into the nature of geometric conservation. It is shown that the flow equations can be written such that time derivatives of integrals over moving domains are avoided prior to discretization. The geometric conservation law is introduced into the equations and the resulting formulation is discretized in time and space without loss of stability and accuracy compared to the fixed grid version. There is no need for temporal averaging remaining. The formulation applies equally to different time integration schemes within a finite element context. Copyright © 2005 John Wiley & Sons, Ltd.

KEY WORDS: DGCL; GCL; time discretization; ALE; deforming domain; second-order time accuracy

1. INTRODUCTION

Robust and accurate time integration on moving domains, treated by means of ALE formulations is a persistent matter of interest [1]. In particular it has been found that the mesh movement has to fulfil special conditions in order to maintain the accuracy and stability of time integration schemes on ALE meshes. Applying these conditions to the fully discretized flow equations results in the so-called discrete geometric conservation laws (DGCL) which have to be fulfilled in order to obtain at least first-order accuracy in time [2]. Furthermore, satisfying the DGCL is suspected to be necessary to guarantee temporal stability in some sense [3] while this point appears to remain controversial [4].

*Correspondence to: Ch. Förster, University of Stuttgart, Institute of Structural Mechanics, Pfaffenwaldring 7, 70550 Stuttgart, Germany.
†E-mail: foerster@statik.uni-stuttgart.de
‡E-mail: wall@lnm.mw.tum.de
§E-mail: eramm@statik.uni-stuttgart.de

Contract/grant sponsor: Deutsche Forschungsgemeinschaft (DFG); contract/grant numbers: SFB 404, TP B4

Received 21 March 2005
Revised 23 August 2005
Accepted 24 August 2005

A DGCL demands for grid positions and velocities computed such that a constant solution can be reproduced exactly. Within finite volume calculations this results in the requirement that the change in size (area or volume in 2D or 3D, respectively) of a cell equals the sum of the respective position changes of the single sides (edges or facets). In the finite element context however no such clear meaning of geometric conservation has been stated [5].

The demand for geometric conservation arises from the fact that the ALE form of the transient balance equation of linear momentum contains a time derivative of an integral term over a deforming domain. Applying time discretization to this integral term results in the question for the proper time instants for evaluating the mass matrices and fluxes and leads to some temporal averaging of these values [3, 6, 7].

An alternative way circumventing the mentioned difficulties is given here. Introducing the geometric conservation law into the derivation of the ALE form, the equation can be written with the time derivative operating on the velocity vector only rather than on the entire integral term. Hence time integration is performed in a straightforward manner and the need for subsequent improvements ensuring geometric conservation is avoided. It is shown that the so-derived discrete equations have to be integrated over the actual domain at time level $n+1$ in order to retain deformation independent results.

The proposed changes have to be performed on the original continuum equations and do not affect the choice of the discretization. Thus the formulation does not cause additional numerical effort. Within this paper the incompressible Navier–Stokes equations are used as an example of a general flow problem and the discretization is performed by means of one-step θ and BDF2 in time while stabilized finite elements are used for spatial discretization. Thus first- and second-order time discretization are covered. Exact satisfaction of the geometric conservation law circumvents limitations on the time step that may emerge otherwise [8].

The reminder of this note gives a brief review of the derivation of the ALE form of the incompressible Navier–Stokes equations in Section 2. The discretization of the resulting equation is described in Section 3 and Section 4 offers a discussion of the geometric conservation properties of the recommended procedure. In Section 5 numerical examples are given confirming the results presented.

2. DERIVATION OF THE ALE FORM OF THE NAVIER–STOKES EQUATIONS

The following derivation applies to all flow equations that can be written on Eulerian meshes in the form

$$\left.\frac{\partial \mathbf{u}}{\partial t}\right|_{\mathbf{x}} + \nabla \cdot \mathbf{F} = \mathbf{f} \tag{1}$$

where $\mathbf{u}$ denotes the velocity vector, $\mathbf{F}$ represents stresses and $\mathbf{f}$ is the body force vector both divided by the fluid density. The time derivative of the velocity is evaluated in the spatial system of reference $\mathbf{x}$ as indicated by $|_{\mathbf{x}}$. The following derivation shall be performed using the Navier–Stokes equations which are one example of class (1) augmented by an algebraic

constraint. In Eulerian formulation the Navier–Stokes equations read

$$\left.\frac{\partial \mathbf{u}}{\partial t}\right|_{\mathbf{x}} + \boldsymbol{\nabla} \cdot (\mathbf{u} \otimes \mathbf{u}) - 2\nu \boldsymbol{\nabla} \cdot \boldsymbol{\varepsilon}(\mathbf{u}) + \boldsymbol{\nabla} p = \mathbf{f} \tag{2}$$

$$\boldsymbol{\nabla} \cdot \mathbf{u} = 0 \tag{3}$$

where ν denotes the kinematic viscosity and $\boldsymbol{\varepsilon}(\mathbf{u}) = \frac{1}{2}(\boldsymbol{\nabla}\mathbf{u} + (\boldsymbol{\nabla}\mathbf{u})^{\mathrm{T}})$ the strain rate tensor. The balance of linear momentum (2) is valid on a possibly deforming configuration which coincides at any $t \in \mathbf{T} = (0, T)$ with the bounded region Ω_t in $\mathbb{R}^m$, $m = 2, 3$ having sufficiently smooth boundary Γ. The boundary can be decomposed into Γ_{N} and Γ_{D} carrying Neumann and Dirichlet boundary conditions, respectively. The Eulerian coordinate system is represented by $\mathbf{x}$ while $\boldsymbol{\chi}$ denotes the ALE coordinate system which tracks the moving boundaries of Ω_t and is allowed to move arbitrarily and independent of the fluid flow inside the domain as indicated in Figure 1. There exists a mapping $\mathbf{x} = \varphi(\boldsymbol{\chi}, t)$ for all $t \in \mathbf{T}$ which is always unique. The reference system $\boldsymbol{\chi}$ can be identified with a particular temporal configuration for example the initial configuration Ω_0. After discretization it is also possible to take the element parameter space for reference.

The particle velocity is given as a function of space and time as $\mathbf{u} = \mathbf{u}(\mathbf{x}, t)$. The Reynolds transport theorem for a function $f(\mathbf{x}, t)$ formulated in an arbitrarily moving frame of reference reads [9]

$$\left.\frac{\partial}{\partial t}\right|_{\boldsymbol{\chi}} \int_{V_t} f(\mathbf{x}, t)\, \mathrm{d}V_t = \int_{V_t} \left.\frac{\partial f(\mathbf{x}, t)}{\partial t}\right|_{\mathbf{x}} \mathrm{d}V_t + \int_{\Gamma_t} f(\mathbf{x}, t) \left.\frac{\partial \mathbf{x}}{\partial t}\right|_{\boldsymbol{\chi}} \cdot \mathbf{n}\, \mathrm{d}\Gamma_t \tag{4}$$

The arbitrary volume V_t occupies a domain which is constant when measured in the reference system $\boldsymbol{\chi}$ and moves with the velocity of the reference system $\mathbf{u}^{\mathrm{G}}(\mathbf{x}, t) = \frac{\partial \mathbf{x}}{\partial t}|_{\boldsymbol{\chi}}$, to be identified with the grid velocity after discretization. Applying (4) to the velocity field and using Gauss divergence theorem on the surface integral leads to

$$\left.\frac{\partial}{\partial t}\right|_{\boldsymbol{\chi}} \int_{V_t} \mathbf{u}(\mathbf{x}, t)\, \mathrm{d}V_t = \int_{V_t} \left.\frac{\partial \mathbf{u}(\mathbf{x}, t)}{\partial t}\right|_{\mathbf{x}} \mathrm{d}V_t + \int_{V_t} \boldsymbol{\nabla} \cdot (\mathbf{u}(\mathbf{x}, t) \otimes \mathbf{u}^{\mathrm{G}}(\mathbf{x}, t))\, \mathrm{d}V_t \tag{5}$$

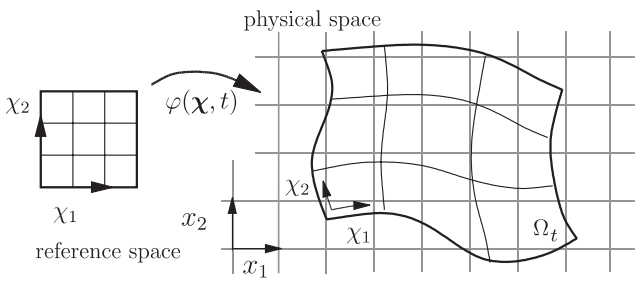

Figure 1. Sketch of ALE measuring of the fluid domain.

The spatial time derivative of $\mathbf{u}$ in (5) is now replaced by means of (2) yielding the linear momentum balance in a deforming reference system

$$\left.\frac{\partial}{\partial t}\right|_{\boldsymbol{\chi}} \int_{V_t} \mathbf{u}\,\mathrm{d}V_t + \int_{V_t} \{\boldsymbol{\nabla}\cdot(\mathbf{u}\otimes(\mathbf{u}-\mathbf{u}^{\mathrm{G}})) - 2\nu\boldsymbol{\nabla}\cdot\boldsymbol{\varepsilon}(\mathbf{u}) + \boldsymbol{\nabla}p\}\,\mathrm{d}V_t = \int_{V_t} \mathbf{f}\,\mathrm{d}V_t \tag{6}$$

where the argument of the velocity has been omitted for brevity. The local form of Equation (6) is widely used for direct discretization [2–4, 7, 8] but leads to the question for the proper time discretization of the first term and consequently to temporal averaging approximating the correct temporal behaviour. The reason for the emerging difficulties is the time derivative of an integral over a temporally dependent domain which cannot be cast into the form $\partial\mathbf{u}/\partial t = f(\mathbf{u}, t)$. Motivated by the successful time integration on Lagrangian meshes commonly performed in continuum solid mechanics we introduce the mapping to the reference position of the deforming frame of reference via the Jacobian determinant

$$J_t = \det\left(\frac{\partial\mathbf{x}}{\partial\boldsymbol{\chi}}\right) \tag{7}$$

which is always positive. The volume element $\mathrm{d}V_t$ can now be replaced by $J_t\,\mathrm{d}V_0$ where V_0 denotes the volume in the reference system, i.e. measured in $\boldsymbol{\chi}$ coordinates. With the time dependence of the domain carried by the scalar Jacobian equation (6) reads

$$\int_{V_0} \left.\frac{\partial(\mathbf{u}J_t)}{\partial t}\right|_{\boldsymbol{\chi}} \mathrm{d}V_0 + \int_{V_0} \{\boldsymbol{\nabla}\cdot(\mathbf{u}\otimes(\mathbf{u}-\mathbf{u}^{\mathrm{G}})) - 2\nu\boldsymbol{\nabla}\cdot\boldsymbol{\varepsilon}(\mathbf{u}) + \boldsymbol{\nabla}p\}J_t\,\mathrm{d}V_0 = \int_{V_0} \mathbf{f}J_t\,\mathrm{d}V_0 \tag{8}$$

Special attention is now turned to two terms. The first term is the time derivative

$$\left.\frac{\partial(\mathbf{u}J_t)}{\partial t}\right|_{\boldsymbol{\chi}} = \frac{\partial\mathbf{u}}{\partial t}J_t + \frac{\partial J_t}{\partial t}\mathbf{u} \tag{9}$$

while the second is the convective term. Using the fact that the velocity field $\mathbf{u}$ is divergence free as Equation (3) demands, differentiation yields

$$J_t\boldsymbol{\nabla}\cdot(\mathbf{u}\otimes(\mathbf{u}-\mathbf{u}^{\mathrm{G}})) = J_t(\mathbf{u}-\mathbf{u}^{\mathrm{G}})\cdot\boldsymbol{\nabla}\mathbf{u} - J_t\boldsymbol{\nabla}\cdot\mathbf{u}^{\mathrm{G}}\mathbf{u} \tag{10}$$

The time derivative of a Jacobian is known from continuum mechanics (see e.g. Reference [10]) to hold

$$\frac{\partial J_t}{\partial t} = J_t\boldsymbol{\nabla}\cdot\mathbf{u}^{\mathrm{G}} \tag{11}$$

Since the Jacobian $J_t = \mathrm{d}V_t/\mathrm{d}V_0$ describes the ratio between differential volume elements in the actual and referential configuration equation (11) gives the relationship of volume transformation and relative velocity between the two systems $\boldsymbol{\chi}$ and $\mathbf{x}$.

Inserting the derivatives (9) and (10) back into (8) and using (11) yields a form of the ALE equation where the time derivative applies to the velocity field only

$$\int_{V_0} \left.\frac{\partial\mathbf{u}}{\partial t}\right|_{\boldsymbol{\chi}} J_t\,\mathrm{d}V_0 + \int_{V_0} \{(\mathbf{u}-\mathbf{u}^{\mathrm{G}})\cdot\boldsymbol{\nabla}\mathbf{u} - 2\nu\boldsymbol{\nabla}\cdot\boldsymbol{\varepsilon}(\mathbf{u}) + \boldsymbol{\nabla}p\}J_t\,\mathrm{d}V_0 = \int_{V_0} \mathbf{f}J_t\,\mathrm{d}V_0 \tag{12}$$

A local ALE form of the Navier–Stokes equations that does not contain Jacobians any more can now be recovered. The time derivative in (12) describes the temporal change of velocity that a reference point $\boldsymbol{\chi}$ experiences while all spatial derivatives refer to the fixed system $\mathbf{x}$.

$$\left.\frac{\partial \mathbf{u}}{\partial t}\right|_{\boldsymbol{\chi}} + (\mathbf{u}-\mathbf{u}^{\mathrm{G}})\cdot\nabla\mathbf{u} - 2\nu\nabla\cdot\boldsymbol{\varepsilon}(\mathbf{u}) + \nabla p = \mathbf{f} \quad \text{in } \Omega_t \times \mathbf{T}$$
$$\nabla\cdot\mathbf{u} = 0 \quad \text{in } \Omega_t \times \mathbf{T} \tag{13}$$

Equation (12) can be understood either as an integral over the current configuration or rather as one over the referential domain V_0 where the single terms are scaled by a time dependent scalar function $J_t(\mathbf{x},t)$. The latter interpretation eases correct discretization and is therefore preferred.

3. DISCRETIZATION

The local form (13) is discretized in time first. Its straightforward temporal discretization inherits the full accuracy and stability properties the time integration scheme offers. To keep track of the changing volume, the Jacobian in (12) is purposefully kept and carried through the discretization. To this end the local momentum balance is written

$$\left.\frac{\partial \mathbf{u}}{\partial t}\right|_{\boldsymbol{\chi}} = \frac{1}{J_t}\{-(\mathbf{u}-\mathbf{u}^{\mathrm{G}})\cdot\nabla\mathbf{u}\,J_t + 2\nu\nabla\cdot\boldsymbol{\varepsilon}(\mathbf{u})J_t - \nabla p\,J_t + \mathbf{f}\,J_t\} \quad \text{in } \Omega_t \times \mathbf{T} \tag{14}$$

Either one-step θ time integration or second-order backward differentiation (BDF2) is used to sample. For a general first-order differential equation $\dot{y} = f(y,t)$ one-step θ time integration yields

$$\frac{y^{n+1}-y^n}{\Delta t} = \theta f(y^{n+1},t^{n+1}) + (1-\theta)\,f(y^n,t^n) \tag{15}$$

while time discretization of the model equation via BDF2 is done via

$$\frac{y^{n+1}-y^n}{\Delta t} = \frac{1}{3}\,\frac{y^n-y^{n-1}}{\Delta t} + \frac{2}{3}\,f(y^{n+1},t^{n+1}) \tag{16}$$

Applying (15) and (16) to the strong form (14) yields

$$\mathbf{u}^{n+1}J_{n+1} + \delta J_{n+1}[(\mathbf{u}^{n+1}-\mathbf{u}^{\mathrm{G},n+1})\cdot\nabla\mathbf{u}^{n+1} - 2\nu\nabla\cdot\boldsymbol{\varepsilon}(\mathbf{u}^{n+1}) + \nabla p^{n+1}] = \mathbf{r}\,J_{n+1} \tag{17}$$

where δ represents a scalar depending on the discretization scheme.

$$\delta_\theta = \theta\Delta t, \quad \delta_{\mathrm{BDF2}} = \tfrac{2}{3}\,\Delta t$$

The vector valued function $\mathbf{r}$ contains a history of the velocity depending on the time integration scheme. Possible body forces $\mathbf{f}$ are also included in $\mathbf{r}$.

$$\mathbf{r}_\theta = \delta_\theta\mathbf{f}^{n+1} + (1-\theta)\,\Delta t\,\dot{\mathbf{u}}^n + \mathbf{u}^n \quad \mathbf{r}_{\mathrm{BDF2}} = \delta_{\mathrm{BDF2}}\,\mathbf{f}^{n+1} + \tfrac{4}{3}\,\mathbf{u}^n - \tfrac{1}{3}\,\mathbf{u}^{n-1}$$

The temporally discretized equation (17) is now discretized in space by means of finite elements. The domain Ω_t is divided into non-overlapping patches, the elements. The spatial discretization maintains its topology while following the deformation of the domain.

To define the Galerkin form we select the finite element spaces $\mathbb{V}_{0,t}^h \subset \mathbb{H}_0^1(\Omega_t)$ and $\mathbb{V}_t^h \subset \mathbb{H}^1(\Omega_t)$, where $\mathbb{V}_t^h$ satisfies the time dependent Dirichlet boundary conditions of the problem while all functions in $\mathbb{V}_{0,t}^h$ are zero on Γ_D. The pressure is taken from the space $P_t^h \subset L_0^2(\Omega_t)$ of square integrable functions with vanishing mean to account for the free additive constant of the pressure variable.

The discrete variational statement is as follows: seek $\mathbf{u} \in \mathbb{V}_{n+1}^h$, $p \in P_{n+1}^h$ such that

$$B(\{\mathbf{u}, p\}, \{\mathbf{v}, q\}) = (\mathbf{r}, \mathbf{v}) + (\mathbf{h}^{n+1}, \mathbf{v})_{\Gamma N, n+1} \quad \forall (\mathbf{v}, q) \in (\mathbb{V}_{0,n+1}^h, P_{n+1}^h) \tag{18}$$

where the discrete operator $B(\{\mathbf{u}, p\}, \{\mathbf{v}, q\})$ is given by

$$B(\{\mathbf{u}, p\}, \{\mathbf{v}, q\}) = (\mathbf{u}, \mathbf{v}) + (\delta(\mathbf{u} - \mathbf{u}^{G,n+1}) \cdot \boldsymbol{\nabla}\mathbf{u}, \mathbf{v}) + (\delta 2\nu\boldsymbol{\varepsilon}(\mathbf{u}), \boldsymbol{\varepsilon}(\mathbf{v})) - (\delta p, \boldsymbol{\nabla} \cdot \mathbf{v}) \tag{19}$$

Here $(\cdot, \cdot)$ denotes the L^2 inner product on the actual mesh configuration Ω_{n+1} if not indicated otherwise and $\mathbf{h}^{n+1}$ represents Neumann boundary forces at the time instant $t = t^{n+1}$.

It is a well known matter of fact that the Galerkin form (18) is ill posed due to the inf–sup condition in the case of finite elements with equal polynomial order in $\mathbb{V}_t^h$ and P_t^h defined on the same triangulation. To stabilize artificial pressure modes as well as oscillations due to convection, residual based stabilization of the unusual type and related to bubble functions as described in References [11, 12] is applied.

4. GEOMETRIC CONSERVATION

It appears interesting to discuss the described method in the light of geometric conservation. The geometric conservation law demands a numerical scheme to reproduce a constant solution exactly and independently of the mesh motion. A temporal and spatial constant velocity field is accompanied by a pressure field that carries the body forces. It is obvious that the time discretized equation (17) is geometrically conserving without any further action required.

To show that geometric conservation is assured in the discrete form a spatial and temporal constant solution $\mathbf{u}$ is inserted into the discrete form (18). Depending on the time discretization scheme this yields

$$(\mathbf{u}^{n+1}, \mathbf{v})_{\Omega_t} = (\mathbf{u}^n, \mathbf{v})_{\Omega_t} \quad \text{and} \quad (\mathbf{u}^{n+1}, \mathbf{v})_{\Omega_t} = \left(\tfrac{4}{3}\mathbf{u}^n, \mathbf{v}\right)_{\Omega_t} - \left(\tfrac{1}{3}\mathbf{u}^{n-1}, \mathbf{v}\right)_{\Omega_t} \tag{20}$$

for one-step θ and BDF2, respectively. Thus geometric conservation requires that at least all mass like terms in (17) have to be integrated over the same domain Ω_t, i.e. at the same instant in time. This agrees with the Galerkin weighted residual procedure which requires the same weighting functions for all residual terms. So Equation (17) has to be tested and integrated within the same configuration in time.

Since the fully discretized equations (18) are solved for the fields of velocity and pressure at the new time level $n+1$, this time level is also chosen for spatial integration. This choice was also indicated by the Jacobians involved in Equation (17). Numerical investigations confirm the choice of the actual configuration t^{n+1} as optimal.

For the solution of the nonlinear variational problem it is assumed that the new mesh configuration Ω_{n+1} as well as the corresponding mesh velocity field $\mathbf{u}^{G,n+1}$ are known. *It is then essential that the mesh motion and position satisfy Equation* (11) *exactly*. Within numerical implementations usually the new mesh position is obtained from a mesh moving

algorithm. It is thus possible to calculate the mesh velocity field such that (11) is satisfied. Since the mesh is not a physical object, i.e. there is no inertia in its motion, it appears sufficient to define a constant velocity over the time interval t^n to t^{n+1} after the new mesh position has been determined. Hence the mesh velocity can be obtained from discrete mesh positions via

$$\mathbf{u}^{\mathrm{G},n+1} = \frac{\mathbf{x}^{n+1} - \mathbf{x}^n}{\Delta t} \tag{21}$$

Using the stepwise constant mesh velocity (21) however does not allow to recover the second-order time accuracy of the BDF2 time stepping scheme. This loss of accuracy occurs because time step refinement also results in a different temporal behaviour of the mesh velocity (another step function) which changes the operator whose solution is sought.

To ensure second-order accuracy in time the temporal interpolation of the mesh motion has to converge at the same rate as the overall algorithm does when the time step is refined. The mesh motion is governed by the first-order differential equation

$$\dot{\mathbf{x}} = \mathbf{u}^{\mathrm{G}} \tag{22}$$

which not only satisfies the geometric conservation law (11) but also is the stronger condition for the mesh movement. Equation (22) can be discretized in time using the same discretization scheme that is applied to the flow problem, i.e. using

$$\frac{\mathbf{x}^{n+1} - \mathbf{x}^n}{\Delta t} = \theta \mathbf{u}^{\mathrm{G},n} + (1-\theta)\mathbf{u}^{\mathrm{G},n+1} \quad \text{and} \quad \frac{\mathbf{x}^{n+1} - \mathbf{x}^n}{\Delta t} = \frac{1}{3}\,\frac{\mathbf{x}^n - \mathbf{x}^{n-1}}{\Delta t} + \frac{2}{3}\,\mathbf{u}^{\mathrm{G},n+1} \tag{23}$$

for one-step θ and BDF2, respectively. Setting $\theta = 0$ in the first equation of (23) recovers Equation (21) which means a constant mesh velocity within a time step following Equation (21) can be interpreted as backward Euler time discretization of the mesh motion (22). Both ways of discretizing (22) in time satisfy the geometric conservation condition (11).

Using the spatial time derivative of a function φ in a moving frame of reference

$$\dot{\varphi} + u^{\mathrm{G}}\varphi_{,x} = 0 \quad \text{with} \quad u^{\mathrm{G}} = \dot{x} \tag{24}$$

as a model problem the local truncation error of the fully discretized schemes can be obtained. This investigation confirms that a temporal discretization of the mesh movement (22) which is second-order allows to obtain second-order accuracy in time for the overall problem also. Numerical investigations confirm these observations.

By choosing (12) rather than (6) for discretization, temporal averaging as reported in References [2–4, 7, 8] is avoided along with the need for introducing DGCLs after discretization. To ensure geometric conservation the algorithm has to be constructed from Equation (12) and has to respect the following:

(i) All spatial integrals have to be evaluated at the same time level.
(ii) The time level to integrate is the one at which the new solution is sought. In the case of one-step θ and BDF2 this is the new time instant $n+1$.

To further transfer the level of accuracy to the moving mesh scheme

(iii) the temporal discretization of the mesh motion (22) has to have the same temporal order of accuracy as the overall algorithm.

Introducing Equation (11) prior to discretization and ensuring it in the discrete equations guarantees geometric conservation and eliminates the necessity of subsequent improvements.

5. NUMERICAL INVESTIGATIONS

The stabilized weak form equation (18) has been consistently linearized and solved via Newton's method.

In order to confirm the choice of the time level $n+1$ for integration an academic two field problem consisting of a fluid and an ALE field is considered as depicted in Figure 2. Nine noded quadratic elements (`quad9` for velocity and pressure) are used in order to avoid inconsistencies inherent in linear elements when combined with residual based stabilization [13]. Higher order elements do not exhibit this type of possible stabilization caused errors.

In order to check the algorithm the pressure value at the mid point M of the domain with the spatial coordinates $(1.0; 0.5)$ is used. The pseudo stationary problem is integrated in time with a time step of $\Delta t = 0.05$. The vertical middle line of the mesh is moved horizontally where the time dependent elongation is given by $x_h = 0.8 \sin(\frac{\Pi}{2} t)$ changing between the positions $+0.8$ and -0.8 with respect to its original location. The starting mesh and the left and right extreme positions are depicted in Figures 3(a), 3(b) and 3(c), respectively. Correct time integration ensures the pressure to be independent of the mesh position or velocity. The problem is solved by one-step θ method and BDF2. When the spatial integration is performed over the domain

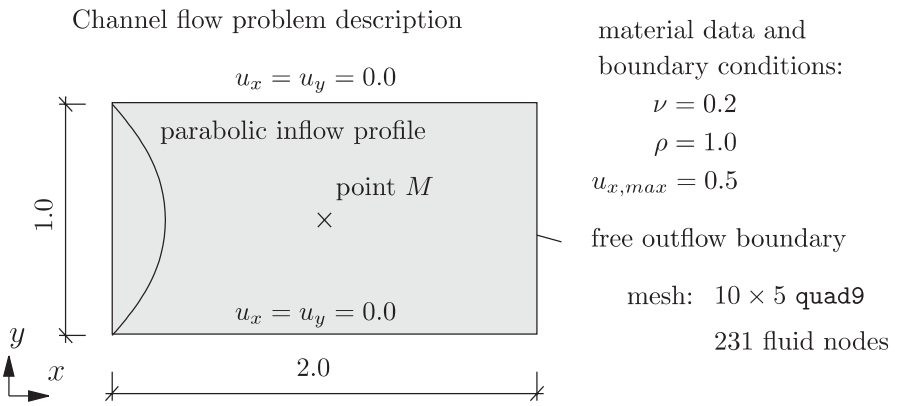

Figure 2. Channel flow example—problem description.

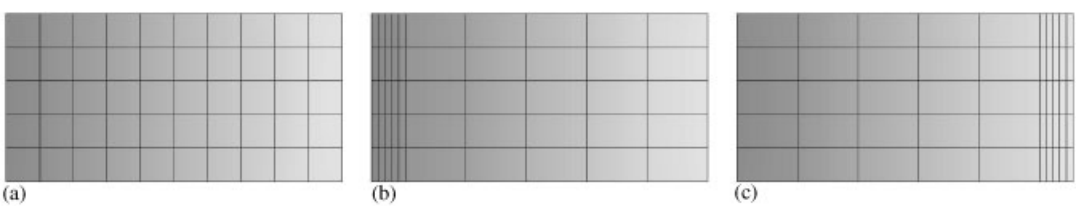

Figure 3. Initial mesh (a) and maximal mesh deformations (b), (c) shown on pressure field.

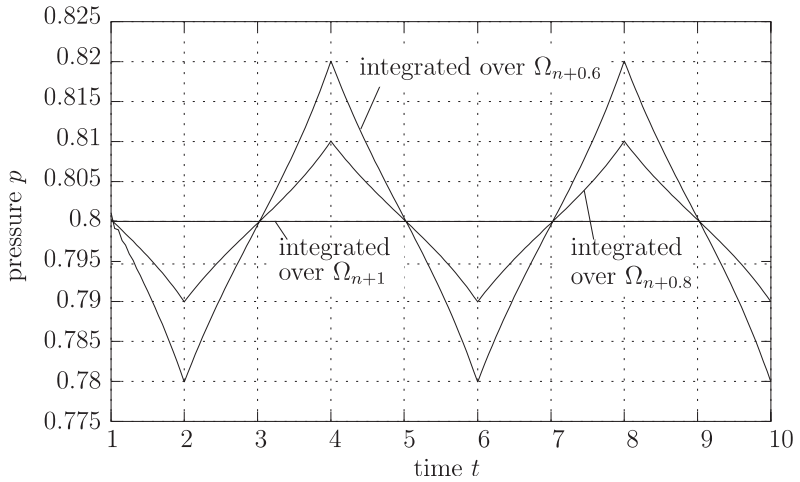

Figure 4. Pressure at mid point M for different integration domains.

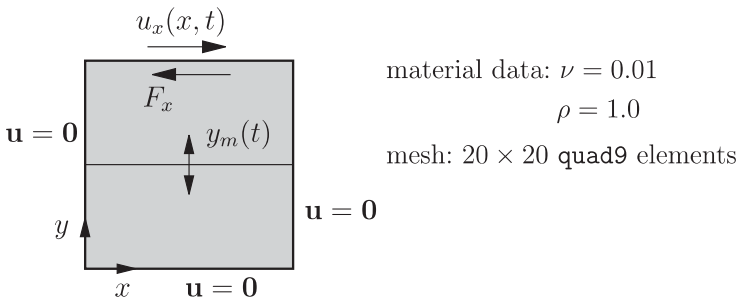

Figure 5. Driven cavity flow example—problem description.

at the new time level $t = t^{n+1}$ both discretization methods give a pressure value at M which is perfectly independent of the mesh motion. The pressure at M remains constant irrespective of θ as indicated by the horizontal line in Figure 4. It may however be tempting for one-step θ calculations at least to use the intermediate time level at $t = t^{n+\theta}$ rather than the new time instant. As shown earlier in (20) this does not violate the geometric conservation law. The pressure result at point M for integration over these time levels for $\theta = 0.6$ and $\theta = 0.8$ is depicted in Figure 4 as well. It shows a clear violation of the expected constant value as soon as one deviates from integrating over Ω_{n+1}. The pressure difference to the correct value in Figure 4 does not depend on the mesh density provided a sufficient resolution is ensured. The error depends however on the deviation of the integration domain $\Omega_{n+\theta}$ from the optimal Ω_{n+1}, i.e. it depends on the time step size and the mesh velocity.

In order to show that second-order accuracy in time can be obtained from the discrete formulation described a second example is investigated. The problem is the well known driven cavity flow where the parameters used here are given in Figure 5. The cavity occupies the unit square and the horizontal flow in x-direction prescribed on the top is parabolic in space and follows a

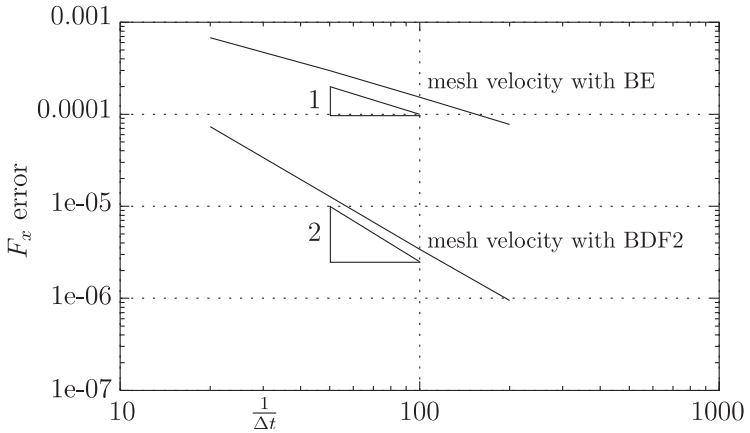

Figure 6. Error in horizontal reaction force.

sinusoidal function in time as $u_x(x,t) = 4(x - x^2)\sin(\frac{\Pi}{4}t)$. For the same reasons as mentioned above quadratic elements in space are used. To investigate a moving mesh, the horizontal mesh middle line as indicated in Figure 5 is moved vertically following $y_m(t) = 0.35\ \sin(\frac{\Pi}{2}t)$. The convergence of the horizontal reaction force F_x at the top of the cavity at time $t = 1.0$ is investigated for different temporal discretizations of the mesh velocity $\mathbf{u}^{\mathrm{G}}$. For both lines in Figure 6 the overall time stepping scheme has been BDF2. The figure shows that using constant mesh velocities within the single time steps effectively sacrifices one order of temporal accuracy. Using a second-order accurate scheme to obtain the new grid velocity restores the overall temporal convergence to second-order on moving meshes without introducing extra effort. The analysis indicates that it should be possible to use the trapezoidal rule ($\theta = \frac{1}{2}$) for the mesh movement while using BDF2 for the solution of the Navier–Stokes equations and still obtain second-order convergence. The trapezoidal rule however tends to introduce oscillations into the scheme. It is therefore recommended to use the second equation of (23) to obtain the new mesh velocity $\mathbf{u}^{\mathrm{G},n+1}$.

The formulation has also been used for the simulation of fluid–structure interaction problems and has shown to be stable and offers accurate results.

6. SUMMARY AND CONCLUSIONS

Introducing the geometric conservation law *a priori* into the derivation of the ALE form of the incompressible Navier–Stokes equations yields a significant simplification of the equations to discretize. The time derivative of an integral term over a temporally changing spatial domain can thus be avoided. The resulting equation can be discretized in time and space straightforwardly without loss of stability and accuracy compared to its fixed grid counterpart provided the temporal discretization of the mesh motion is of the same order as the overall algorithm. No additional complexity is introduced.

The formulation allows to circumvent temporal averaging of mass terms and fluxes. Since the conservation law is introduced prior to discretization the formulation remains general

and equally applicable to different temporal and spatial discretization schemes. Different discrete geometric conservation laws are avoided. Thus it remains to design mesh positions and velocity such that Equation (11) is satisfied.

Formal application of geometric conservation is not the entire answer to the question of proper time integration on deforming domains. Integrating the correct equations entirely at the wrong time instant results in changing solutions due to mesh movement which can be avoided by choosing the correct domain Ω_{n+1} at actual time $t = t^{n+1}$. It is further essential to discretize the mesh motion (22) in time such that the same order of accuracy is ensured that is used for the overall algorithm. This can effectively be done by using the same temporal discretization scheme for the time discretization of the fluid flow and the mesh positions.

ACKNOWLEDGEMENTS

The present study is supported by a grant of the foundation 'Deutsche Forschungsgemeinschaft' (DFG) under project B4 of the collaborative research centre SFB 404 'Multifield Problems in Continuum Mechanics'. This support is gratefully acknowledged.

REFERENCES

1. Huerta A, Rodriguez-Ferran A (eds). The arbitrary Lagrangian–Eulerian formulation. *Computer Methods in Applied Mechanics and Engineering* 2000; **193**(39–41):4073–4456 (special issue).
2. Guillard H, Farhat C. On the significance of the geometric conservation law for flow computations on moving meshes. *Computer Methods in Applied Mechanics and Engineering* 2000; **190**(11–12):1467–1482.
3. Farhat C, Geuzaine P, Grandmont C. The discrete geometric conservation law and the nonlinear stability of ALE schemes for the solution of flow problems on moving grids. *Journal of Computational Physics* 2001; **174**(2):669–694.
4. Boffi D, Gastaldi L. Stability and geometric conservation laws for ALE formulations. *Computer Methods in Applied Mechanics and Engineering* 2004; **193**(42–44):4717–4739.
5. Wall WA. Fluid-Struktur-Interaktion mit stabilisierten Finiten Elementen. *Ph.D. Thesis*, Institute of Structural Mechanics, University of Stuttgart, 1999.
6. Geuzaine P, Grandmont C, Farhat C. Design and analysis of ALE schemes with provable second-order time-accuracy for inviscid and viscous flow simulations. *Journal of Computational Physics* 2003; **191**(1):206–227.
7. Farhat C, Geuzaine P. Design and analysis of robust ALE time-integrators for the solution of unsteady flow problems on moving grids. *Computer Methods in Applied Mechanics and Engineering* 2004; **193**(39–41): 4073–4095.
8. Koobus B, Farhat C. Second-order time-accurate and geometrically conservative implicit schemes for flow computations on unstructured dynamic meshes. *Computer Methods in Applied Mechanics and Engineering* 1999; **170**(1–2):103–129.
9. Donea J, Huerta A. *Finite Element Methods for Flow Problems*. Wiley: Chichester, 2003.
10. Marsden JE, Hughes TJR. *Mathematical Foundations of Elasticity*. Prentice-Hall: Englewood Cliffs, NJ, 1983.
11. Franca LP, Valentin F. On an improved unusual stabilized finite element method for the advective–reactive–diffusive equation. *Computer Methods in Applied Mechanics and Engineering* 2000; **190**(13–14):1785–1800.
12. Franca LP, Farhat C. Bubble functions prompt unusual stabilized finite element methods. *Computer Methods in Applied Mechanics and Engineering* 1995; **123**(1–4):299–308.
13. Jansen EK, Collis SS, Whiting C, Shakib F. A better consistency for low-order stabilized finite element methods. *Computer Methods in Applied Mechanics and Engineering* 1999; **174**(1–2):153–170.

